INTERNATIONAL JOURNAL FOR NUMERICAL METHODS IN FLUIDS
Int. J. Numer. Meth. Fluids 2009; **61**:291–310
Published online 26 November 2008 in Wiley InterScience (www.interscience.wiley.com). DOI: 10.1002/fld.1958

Opposing mixed convection and its interaction with radiation inside eccentric horizontal cylindrical annulus

Anjan Sarkar[1,*,†], S. K. Mahapatra[2,‡] and A. Sarkar[1]

[1]*Department of Mechanical Engineering, Jadavpur University, Kolkata 700032, West Bengal, India*
[2]*Department of Mechanical Engineering, National Institute of Technology, Quarters No. D/42, N.I.T. Campus, Rourkela 769008, Orissa, India*

SUMMARY

In the present investigation, the coupled phenomenon of opposing mixed convection and radiation within differentially heated eccentric horizontal cylindrical annulus has been numerically simulated. The radiation transfer contributed from the participating medium is obtained by solving the nonlinear integro-differential radiative transfer equation using discrete ordinate method. The participating gray medium is considered to be emitting, absorbing and isotropically scattering. The walls of the annulus are considered to be opaque, diffuse and gray. In the study it has been observed that the Richardson number '*Ri*' has a small effect on the total Nusselt number '*Nu*' in mixed convection heat transfer with or without radiation. From the present investigation it is found that substantial changes occur in isotherms as well as in flow patterns, when the Richardson number is allowed to vary in the range of 0.01–1. The influence of radiative parameters on the interaction phenomenon has been delineated through isotherm and streamline pattern. Copyright © 2008 John Wiley & Sons, Ltd.

Received 10 October 2007; Revised 26 September 2008; Accepted 2 October 2008

KEY WORDS: mixed convection; radiation; participating medium; cylindrical annulus

INTRODUCTION

Mixed convection in a rotating cylindrical annulus has pioneered many engineering industries related to cooling. Many applications are encountered in seeking improvements for crystallographic

*Correspondence to: Anjan Sarkar, Department of Mechanical Engineering, Jadavpur University, Kolkata 700032, West Bengal, India.
†E-mail: anjansirkar@yahoo.com
‡Professor.

perfection in industrial processing, food processing, melting of a phase change material around a heating pipe in a thermal storage system, cooling of electronic components and transmission cables, heat transfer phenomena around nuclear fuel bundles in a nuclear reactor, etc. Owing to its special importance in electronic cooling (for example, a base phone, a mobile phone or a pager), several researchers have studied the entire phenomena either experimentally or computationally to capture the flow and heat transfer characteristics inside an enclosed domain. In the mixed convection system with a fixed radius ratio, the flow and heat transfer characteristics are determined by the Rayleigh number (buoyancy) and Reynolds number (rotation), respectively. To set a control parameter for buoyancy and rotation, a non-dimensional number known as 'Richardson number ($Ri = Gr/Re^2$)' is introduced in this study, which determines the relative importance of buoyancy with respect to rotational effects.

Owing to the simple geometry and well-defined boundary conditions, the analysis of natural convection within cylindrical annuli has been studied extensively by Choudhury and Karki [1]. They studied this problem with eccentricity along the vertical line. In their study, they concluded that the eccentricity introduces additional non-uniformity in the flow and temperature fields. Fusegi *et al.* [2] did not consider eccentric cases but treated the problem for both high and low values of the densimetric Froude number (relative magnitude of buoyancy versus rotational effects). Lee [3] treated the problem over a good range of Rayleigh numbers allowing for both horizontal and vertical eccentricities of the inner cylinder. It was concluded that the mean Nusselt number increased with the Rayleigh number at a given angular velocity and decreased with the rotation speed, keeping other parameters constant. Lee *et al.* [4] used a generalized differential–integral quadrature discretization technique to solve a mixed convection problem inside horizontal eccentric annuli in a body-fitted coordinate system. In their study, they found out that the net circulation decreases and approaches zero with the rise of the Rayleigh number and it reaches its minimum value with high eccentricity when the inclination angle of eccentricity is π. The forced flow due to an unheated rotating cylinder had been studied by Taylor [5] and Coles [6], in which only the centrifugal force was considered, which leads to the Taylor vortices because of the existence of hydrodynamic instability when the Reynolds number reaches a critical value. A comprehensive review of the analytical and experimental investigations for the annulus with a rotating inner cylinder is given by DiPrima and Swinney [7]. Ball and Farouk [8] and Ball [9] undertook a detailed study on the development of Taylor vortices and the distribution of heat transfer in a vertical annulus with a heated rotating inner cylinder. For the vertical orientation (for moderate speeds of rotation), the flow field generated by the centrifugal and the buoyancy effects are both axi-symmetric. For the horizontal configuration, however, the buoyancy and the centrifugal effects will give rise to fully three-dimensional flows when the centrifugal force is strong enough to trigger the formation of Taylor cells.

Some relevant studies related to radiation modeling of participating medium and the interaction phenomenon of radiation with other modes of heat transfer are hereby addressed. Chui and Raithby [10] and Chai *et al.* [11] proposed the finite volume method (FVM) for simulating radiative transfer equation (RTE). This method has been successfully applied to various problems in radiative equilibrium, proving its accuracy in the non-orthogonal as well as in the orthogonal coordinate system. Kim and Baek [12] have also adopted FVM to examine combined heat transfer in a gradually expanding channel, showing that it is compatible with flow solvers, also based on the FVM. Onyegegbu [13] was one of the early researchers to investigate the combined heat transfer problem of a radiatively participating medium within a horizontal annulus. In this study, a finite difference-based iterative method was used along with the Milne–Eddington approximation

DOI: 10.1002/fld

for modeling the radiative transfer. The Milne–Eddington approximation results in a differential equation that is identical to the P_1 approximation. The effect of participating medium radiation on mixed convection phenomenon inside differentially heated square enclosure has also been investigated in the study of Mahapatra *et al.* [14]. In their study they explained how some notable features of radiation (flow reversal, suppression of buoyancy in the core of cavity) affect the opposing mixed convection inside the cavity. Tan and Howell [15] also simulated the horizontal annulus flow using a finite difference method, but they employed the YIX method to handle the integral part of the RTE. Morales and Campo [16] conducted a series of numerical investigations for flows within a horizontal annulus using the P_1 approximation with a control-volume-based finite difference method. Burns *et al.* [17] solved the same problem using a finite element formulation for the combined mode heat transfer. Tan and Howell [15], Morales and Campo [16] and Burns *et al.* [17] all considered the same radius ratio ($\eta = 2.6$), and in all three studies an unusual quadra-cellular flow was obtained as the steady-state solution for $Ra = 10^5$, $NR = 1$, $\tau = 1$. All of the above studies assumed symmetry in vertical mid-plane and solved the two-dimensional steady-state form of the model equations.

The relevant studies cited above reveal that a good amount of investigation has been carried out on natural convection in two-dimensional differentially heated cylindrical annulus. A few researchers have also investigated the coupled phenomenon of natural convection and radiation within different geometrical configurations, employing different radiation modeling schemes. From the above literature review, it can be seen that though a few investigations have been made for pure mixed convection cases inside horizontal cylindrical annulus, no extensive study has been conducted yet with regard to the interaction of medium radiation with mixed convection inside horizontal cylindrical annulus. To provide some light in this regard, the present investigation is made. Furthermore, this study has direct relevance in hybridization oven where two concentric cylinders are retrofitted with a provision of muffin fan. The larger outer cylinder has a dual nature. It directs the flow of air when imparted an angular motion and provides a dielectric shell for safety. In this regard, Stovall Life Science makes hybridization ovens for research and development by molecular biologists on deoxy-ribonucleic acid and ribonucleic acid.

GOVERNING EQUATIONS

The physical model is shown in Figure 1(a). The flow is considered to be two-dimensional, laminar and incompressible and the fluid is considered to be of having constant thermo-physical properties. However, the density variation is assumed as per Boussinesq approximation.

All the governing equations such as continuity, momentum, energy [18] and RTE have been formulated in dimensionless form using the following non-dimensional variables as follows:

$$\psi = \psi_d/\alpha, \quad \Omega = \Omega_d/(\alpha/d^2), \quad \phi = (T - T_o/T_i - T_o), \quad I^* = I/(\sigma T_m^4)$$

The dimensionless forms of all governing equations along with boundary conditions are:

Continuity equation:

$$\nabla^2 \psi = -\Omega \tag{1}$$

DOI: 10.1002/fld

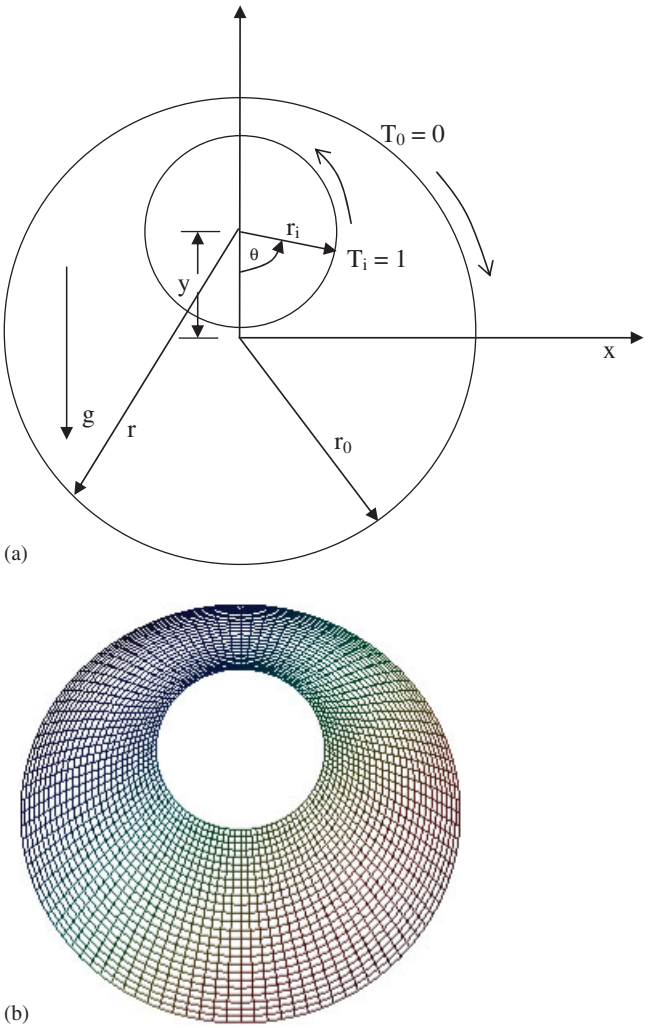

Figure 1. (a) Physical domain and (b) computational domain.

Momentum equation:

$$\nabla^2\Omega = \frac{1}{Pr}\left(U\frac{\partial\Omega}{\partial R} + \frac{V}{R}\frac{\partial\Omega}{\partial\theta}\right) + Ra\left(\cos\theta\frac{\partial\phi}{\partial R} - \frac{\sin\theta}{R}\frac{\partial\phi}{\partial\theta}\right) \tag{2}$$

Energy equation:

$$\nabla^2\phi = U\frac{\partial\phi}{\partial R} + \frac{V}{R}\frac{\partial\phi}{\partial\theta} - C_2\{G - 4(\phi + C_1)^4\} \tag{3}$$

DOI: 10.1002/fld

Table I. Grid independence test.

Fixed parameter	Grid size	Nu_c (hot wall)	Nu_c (cold wall)
$Ra=10^5,\ Pr=0.72$	20×80	3.5319	3.7305
	30×120	3.4693	3.5984
	40×160	3.4517	3.5476
	50×200	3.4237	3.5167
	60×200	3.4195	3.5074
	60×240	3.4121	3.5038

Table II. Variation of (a) 'K_{eq}' with Ra for natural convection and (b) 'K_{eq}' when $Ra=10^5, NR=1, \tau=1$.

Study	$Ra=10^4$	$Ra=10^5$
(a)		
Morales and Campo [16]	1.98	3.47
Present study	2.00	3.51
(b)		
Kuo *et al.* [20]		13.60
Present study		12.98

where

$$C_1=T_0/\Delta T,\quad C_2=NR\cdot ad^2/(r_i\cdot C_1^3),\quad G=\frac{T_m^4}{(T_i-T_o)^4}\int_{4\pi} I^*(R,\hat{s}')\,\mathrm{d}\phi'$$

The boundary conditions are given as

$$\phi=1,\quad \Omega=\frac{\partial V}{\partial R},\quad \psi=0,\quad V=Pr\cdot Re,\quad R=r_i/d,\quad -\pi/2\leqslant\theta\leqslant 3\pi/2$$

$$\phi=0,\quad \Omega=\frac{\partial V}{\partial R},\quad \psi=0,\quad V=-Pr\cdot Re,\quad R=(r_i+d_g)/d,\quad -\pi/2\leqslant\theta\leqslant 3\pi/2$$

where $d_g=(r_o^2-y^2\sin^2\theta)^{1/2}-(r_i-y\cos\theta)$ and 'y' is the distance of eccentricity as shown in Figure 1(a).

U and V are expressed as:

$$U=\frac{1}{R}\frac{\partial\psi}{\partial\theta},\quad V=-\frac{\partial\psi}{\partial R}$$

DOI: 10.1002/fld

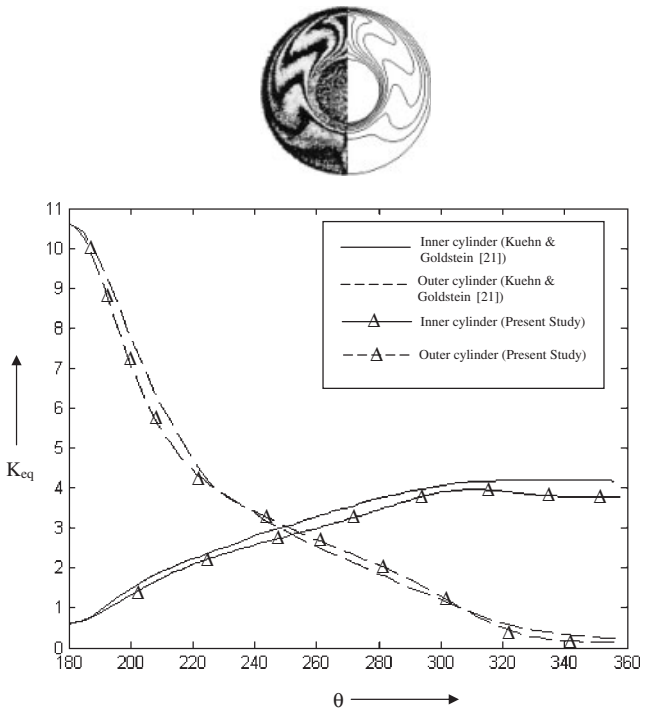

Figure 2. (a) Comparison of isotherm contours of the present study with the experimental study of Kuehn and Goldstein [21] when $Ra = 4.8 \times 10^4$ in the case of pure natural convection and (b) comparison of the present numerical study with the experimental work made by Kuehn and Goldstein [21] against a term 'K_{eq}' with respect to 'θ'.

The RTE for an emitting, absorbing and isotropically scattering gray medium with constant properties is given as

$$\frac{1}{\tau}\frac{\mathrm{d}I^*(R,\hat{s})}{\mathrm{d}s^*} = \frac{(1-\omega)}{\pi}\left(\frac{T_o+\phi\Delta T}{T_m}\right)^4 - I^*(R,\hat{s}) + \frac{\omega}{4\pi}\int_{4\pi} I^*(R,\hat{s}')\xi(\hat{s}',\hat{s})\,\mathrm{d}\Phi' \tag{4}$$

where $\xi(\hat{s}',\hat{s}) = 1$ for isotropic scattering.

The application of discrete ordinate method (DOM) to RTE simplifies source term as $\int f(\hat{s})\,\mathrm{d}\Phi = \sum W_j f(\hat{s}_j)$, where W_j are weight factors associated in the jth direction.

Walls are considered to be gray, diffuse and opaque. The boundary condition is given as

$$I^*(R_w,\hat{s}) = \frac{\varepsilon_w(R_w)}{\pi}\left(\frac{T_o+\phi\Delta T}{T_m}\right)^4 + \frac{1-\varepsilon_w(R_w)}{\pi}\int_{\hat{s}'\cdot\hat{n}_w<0} I^*(R_w,\hat{s}')|\hat{s}'\cdot\hat{n}_w|\,\mathrm{d}\Phi$$

where $\varepsilon_w(R_w)$ and $\hat{n}_w$ denote the wall emissivity and surface unit normal vector, respectively.

As there is no boundary condition available in azimuthal direction, the intensities in discrete directions are calculated from the wall boundary conditions only.

DOI: 10.1002/fld

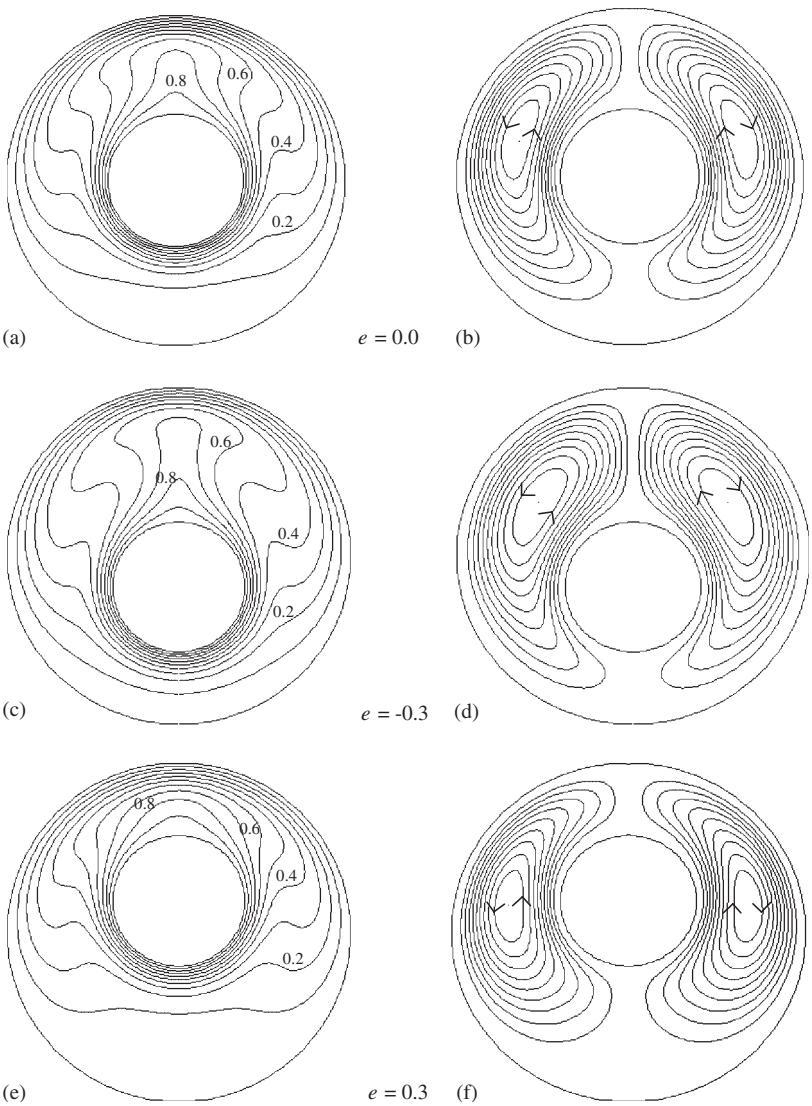

Figure 3. Isotherm and streamline pattern for concentric and eccentric annuli in the case of natural convection when $Ra = 10^4$.

The average Nusselt numbers for convective and radiative heat transfer are calculated as per the following equations:

$$Nu_c = -\left(\sum A_i \frac{\partial T_i}{\partial r}\right) \Big/ \left(2\pi \frac{\Delta T}{\ln(r_o/r_i)}\right)$$

DOI: 10.1002/fld

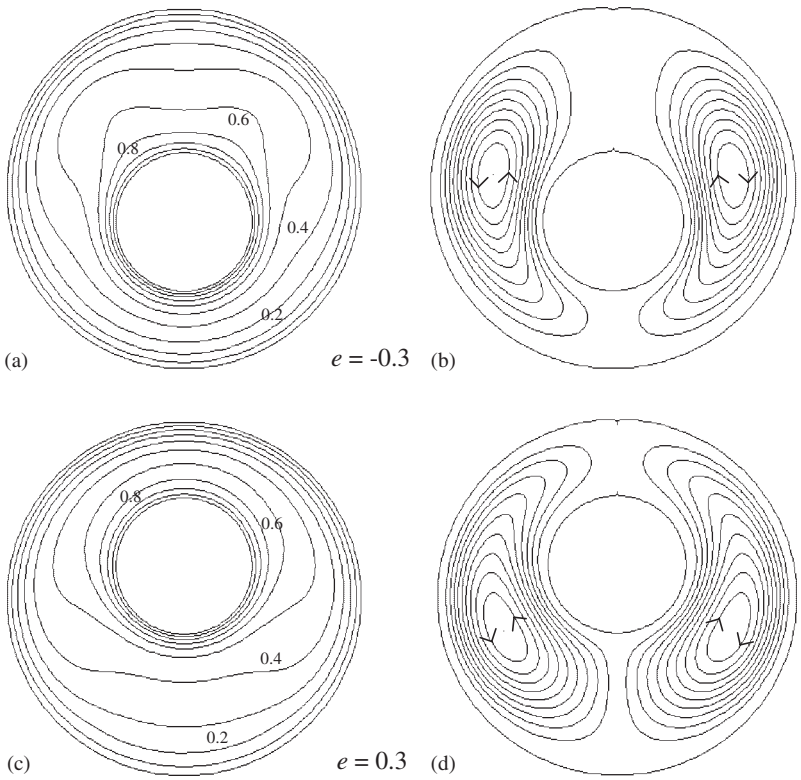

Figure 4. Isotherm and streamline pattern with variation in eccentricity (e) for natural convection and radiation when $NR=1, \tau=1, \omega=0.5, \varepsilon=0.5$ and $Ra=10^4$.

and

$$Nu_r = -\left(\sum A_i \frac{1}{(3-A_1\omega)} \frac{\partial G_d}{\partial \tau}\right) \Big/ \left(2\pi k \frac{\Delta T}{\ln(r_o/r_i)}\right)$$

where $G_d = G \cdot \sigma \cdot (T_i - T_o)^4$.

The total average Nusselt number for either of the inner or outer cylinder wall is calculated as follows:

$$Nu_t = Nu_c + Nu_r$$

NUMERICAL PROCEDURE

Navier–Stokes equations in the cylindrical coordinate system are solved with energy equation and radiative transfer equation inside the computational domain along with their respective boundary conditions. A grid independence test has been conducted for pure natural convection against the value of Nusselt numbers '*Nu*' at both the active walls and is given in Table I. Therefore, a final mesh size of 50×200 in radial and azimuthal directions, respectively, is used for the rest of the

DOI: 10.1002/fld

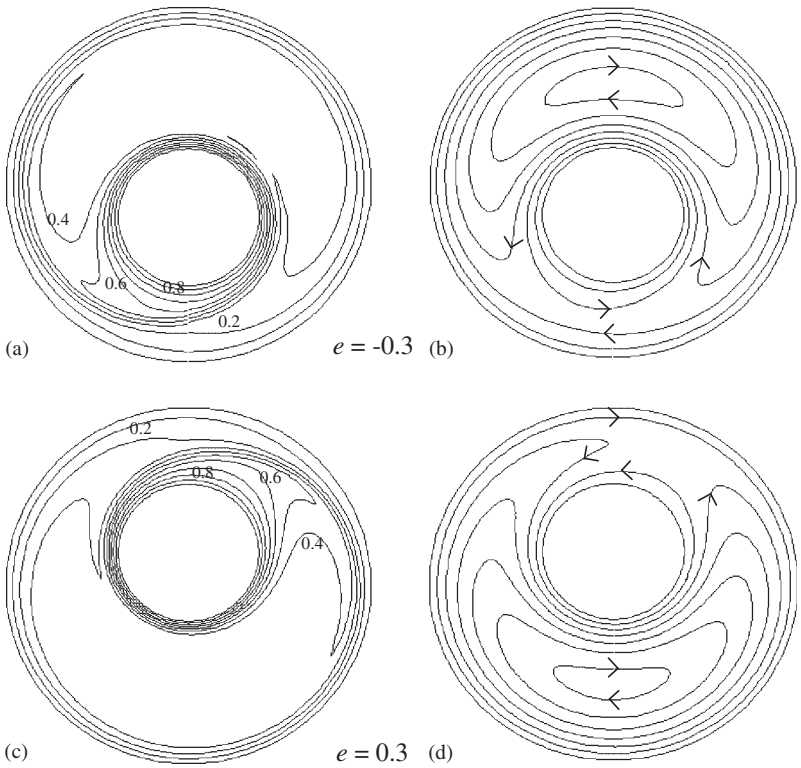

Figure 5. Isotherm and streamline pattern for pure mixed convection with variation in eccentricity (e) when $Ri = 0.01$ and $Ra = 10^4$.

computational efforts. The non-uniform meshing in radial direction (shown in Figure 1(b)) has been done in order to capture the flow structure near the boundary. The nonlinear source term of the vorticity equation and energy equation as well as the second-order partial derivatives present there is discretized by the central difference method. To solve the radiative transfer equation (RTE), the DOM is applied to find out the non-dimensional radiative intensity (I^*) at each grid point. The weight factors along the requisite directions are taken as per S_4 approximation [19]. An initial guess is made for stream-function, vorticity and intensity terms, whereas a conduction temperature field is given as an initial guess for the calculation of the temperature field. Under-relaxation parameters of 0.5 and 0.3 are used for energy equation and vorticity equation, respectively, whereas an over-relaxation parameter of 1.2 is adopted in RTE. Convergence criterion is set at 10^{-7} for all variables for obtaining convergence.

RESULTS AND DISCUSSIONS

As discussed in the last part of the 'Introduction' section, the present numerical study is mainly focused to simulate the case of a hybridization oven; therefore, the ranges of the parameters studied

DOI: 10.1002/fld

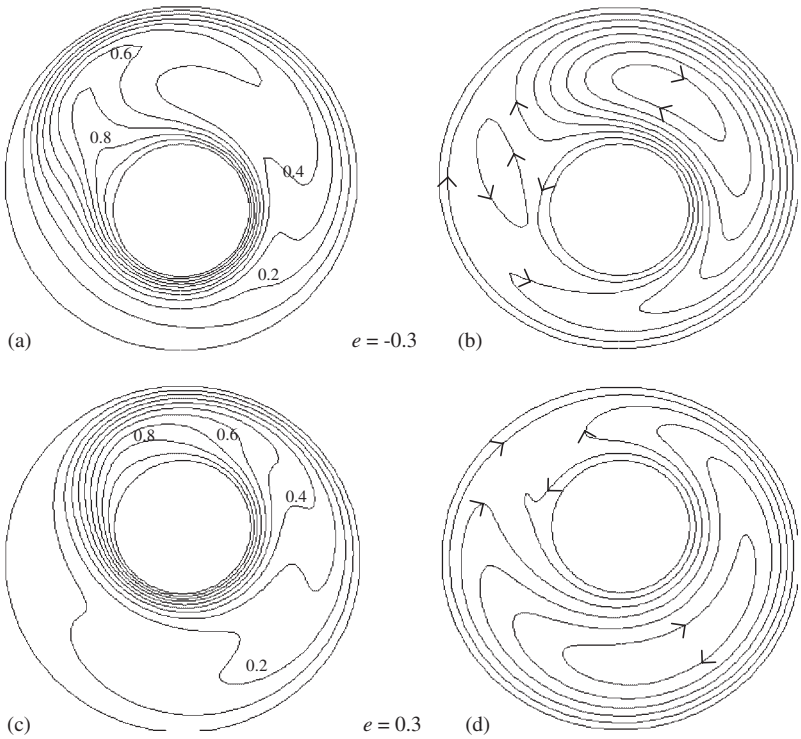

Figure 6. Isotherm and streamline pattern for pure mixed convection with variation in eccentricity (e) when $Ri = 1$ and $Ra = 10^4$.

are restricted within a specified limit to capture the correct thermal and flow behavior inside the oven. In the present study, the inner cylinder is assumed to be at a high temperature, whereas the outer cylinder is kept at a low temperature. This onsets natural convection within the annuli. The position of the inner cylinder is varied by varying the eccentricity (e) along vertical direction only. The inner and outer cylinders are imparted a constant angular velocity in opposite directions, which results in mixed convection phenomenon to occur inside it. The flow is assumed to be invariant along the axis of the cylinders, which leads to a two-dimensional approach. Consequently, with respect to wall movement, the Richardson number (Ri) becomes an influencing parameter in addition to the Rayleigh number (Ra).

The angular motion of the outer cylinder for this type of hybridization oven is roughly 2–15 RPM. Considering this prime aspect, it has been calculated roughly that for a cylinder of approximate diameter ($\leqslant$15 cm) rotating with the above given range of RPM and $Ra = 10^4$, a minimum value of Richardson number (Ri) of 0.01 is obtained. Considering these aspects, the study has been performed for $Ri = 0.01$–1 for the present investigation. Beyond this range of Richardson number (Ri), the variations in isotherms and flow patterns are negligible, which is discussed later. To make a more realistic study on this component, the effect of thermal radiation on mixed convection has been examined thoroughly considering the medium to be absorbing, emitting and diffusely reflecting. Generally, all kinds of hybridization ovens are operated at a

DOI: 10.1002/fld

Table III. Variation of '*Nu*' with respect to '*Ri*' and '*e*' for pure opposing mixed convection.

Fixed parameter	Variable parameter		Nu_c (hot wall)	Nu_c (cold wall)	$\lvert\psi_{max}\rvert$
$Ra=10^4$, $e=-0.5$	*Ri*	0.005	2.1195	2.1865	98.3102
		0.01	2.1126	2.1804	91.6387
		1	1.9259	1.9872	37.7322
		Natural convection	2.1018	2.1321	18.7517
$Ra=10^4$, $e=-0.3$	*Ri*	0.005	2.4397	2.5027	342.0542
		0.01	2.4391	2.5006	316.5004
		1	1.9140	1.9453	37.1467
		Natural convection	2.0486	2.0786	16.3487
$Ra=10^4$, $e=-0.1$	*Ri*	0.005	1.1364	1.1485	86.3756
		0.01	1.1310	1.1451	62.9492
		1	1.8360	1.8962	27.4057
		Natural convection	1.9969	2.0345	14.1563
$Ra=10^4$, $e=0.0$	*Ri*	0.005	0.9972	1.0265	235.6245
		0.01	0.9915	1.0237	211.9379
		1	1.8652	1.9065	28.6451
		Natural convection	1.9485	2.0020	13.066
$Ra=10^4$, $e=0.1$	*Ri*	0.005	1.1097	1.1567	89.3613
		0.01	1.1081	1.1519	66.4659
		1	1.7881	1.8589	24.5493
		Natural convection	1.9162	1.9662	12.4718
$Ra=10^4$, $e=0.3$	*Ri*	0.005	2.4773	2.5381	329.1224
		0.01	2.4729	2.5368	314.7463
		1	1.7229	1.7793	27.7227
		Natural convection	1.7956	1.8603	11.1639
$Ra=10^4$, $e=0.5$	*Ri*	0.005	1.9365	1.9713	78.9723
		0.01	1.9332	1.9698	63.1761
		1	1.6489	1.7176	23.6122
		Natural convection	1.7169	1.7942	9.8570

temperature of below 100°C. From the literature referred in the text, it can be found that in this temperature range the radiative heat transfer is at par with the convective heat transfer. Thus, to simulate this situation the radiation–conduction parameter (i.e. NR) is taken as '1' in the entire study.

Validation with benchmark results

The numerical code developed has been validated against the study of Morales and Campo [16] for natural convection and Kuo *et al.* [20] for natural convection and radiation, when $Ra=10^4$ and 10^5. A term named 'K_{eq}' (ratio of total heat flux through the annulus due to convection and radiation to the heat flux due to conduction only) is found out for validation purpose and presented in Table II. The agreement with earlier studies is quite good and an error of 1.15% is noticed in case of pure natural convection, whereas an error of 4.56% is noticed for the case of natural convection and radiation. The effects of influencing parameters have been analyzed by varying any one parameter and keeping the other parameters fixed. The analysis of natural convection,

DOI: 10.1002/fld

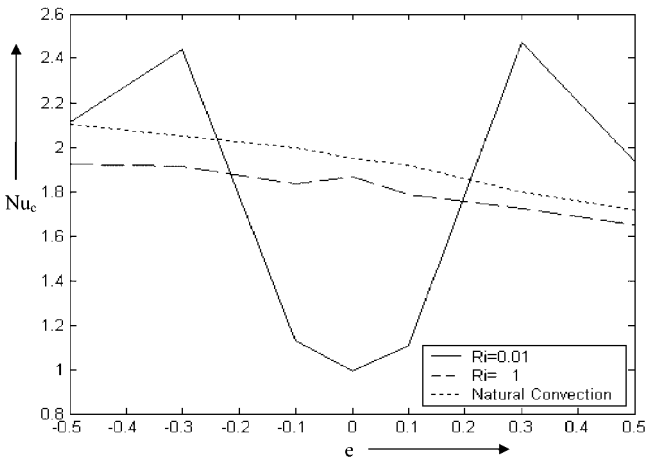

Figure 7. The comparison plots of 'Nu_c' against 'e' for $Ri = 0.01, 1$ (i.e. mixed convection) and natural convection in the absence of radiation.

mixed convection, coupled natural convection and radiation and combined mixed convection and radiation has been made to reveal the physics by understanding different phenomena. Thereby, sole effect due to radiation and eccentricity can be properly identified.

For the sake of authenticity of the code, it is further compared with the experimental results obtained by Kuehn and Goldstein [21] considering the case of pure natural convection only. They carried out the experiment with nitrogen as fluid for two different situations to produce one fringe shift. (i) A temperature difference of 35°C was applied at a pressure of 0.15 atm and (ii) a temperature difference of 0.1°C was applied at a pressure of 35 atm. The fringe pattern obtained for isotherms at a Rayleigh number ($Ra = 4.8 \times 10^4$) inside the concentric cylindrical annuli is compared with the present numerical results for same value of 'Ra' in Figure 2(a). Apart from that, the plot of 'K_{eq}' against 'θ' along the inner and outer cylinders of the concentric annuli has also been compared with the present numerical study. In all locations, both the inner and outer cylinders ensure a good match except the bottom portion of the inner cylinder, where a maximum deviation of 8% is noticed from the experimental work (shown in Figure 2(b)). Keeping an eye on these above-discussed numerical and experimental results, the present numerical study is conducted for two values of Rayleigh number i.e. $Ra = 10^4$ and 10^5.

Natural convection and radiation

Figure 3 shows the isotherm and streamline pattern of pure natural convection for three different eccentricities i.e. $e = 0$, -0.3 and 0.3. For $Ra = 10^4$, referring to Figure 3(b) (i.e. differentially heated concentric cylindrical annulus), a thin thermal boundary layer develops and rises along both sides of the inner cylinder wall, meets at the top of the inner cylinder resulting in a thermal plume and again gets detached on colliding with the outer cylinder. This segregation of the plume forms two counter-rotating cells on two sides of the annulus because of the convective current. The lower half of the annulus is subjected to a conductive heat flow due to the presence of the stagnant fluid. When the position of the inner cylinder shifts downward (i.e. $e = -0.3$), the temperature and

DOI: 10.1002/fld

Table IV. Variation of '*Nu*' with respect to '*Ri*' and '*e*' for opposing mixed convection along with radiation.

Fixed parameter	Variable parameter		Nu_c (hot wall)	Nu_r (hot wall)	Nu_c (cold wall)	Nu_r (cold wall)	$\lvert\psi_{max}\rvert$
$Ra=10^4$, $e=-0.5$, $NR=1$, $\tau=1$, $\varepsilon=0.5$, $\omega=0.5$	Ri	0.01	2.4640	5.8489	3.6818	4.8645	118.8246
		1	2.2548	5.7878	3.3861	4.8375	46.0865
$Ra=10^4$, $e=-0.3$, $NR=1$, $\tau=1$, $\varepsilon=0.5$, $\omega=0.5$	Ri	0.01	2.7322	5.9070	4.0566	4.7955	316.9430
		1	2.1895	5.7952	3.3450	4.7667	39.4479
$Ra=10^4$, $e=-0.1$, $NR=1$, $\tau=1$, $\varepsilon=0.5$, $\omega=0.5$	Ri	0.01	2.0650	5.7618	3.2571	4.7395	79.2383
		1	2.2482	6.1388	2.7132	3.8867	25.7685
$Ra=10^4$, $e=0.0$, $NR=1, \tau=1$, $\varepsilon=0.5$, $\omega=0.5$	Ri	0.01	1.9979	5.7386	3.1871	4.7247	202.2155
		1	2.1288	5.7737	3.3463	4.7283	31.2960
$Ra=10^4$, $e=0.1$, $NR=1, \tau=1$, $\varepsilon=0.5$, $\omega=0.5$	Ri	0.01	2.0337	5.7612	3.2418	4.7192	74.0072
		1	2.1219	5.7999	3.3172	4.6560	30.2283
$Ra=10^4$, $e=0.3$, $NR=1, \tau=1$, $\varepsilon=0.5$, $\omega=0.5$	Ri	0.01	2.7633	5.9118	4.1023	4.7933	314.6016
		1	2.1078	5.7672	3.4068	4.7394	33.3528
$Ra=10^4$, $e=0.5$, $NR=1$, $\tau=1$, $\varepsilon=0.5$, $\omega=0.5$	Ri	0.01	2.4437	5.8853	3.7083	4.7451	87.6732
		1	2.1561	5.8502	3.3575	4.5803	33.3132

flow field are shown through the isotherm and streamline patterns in Figure 3(c) and (d). A large plume exists in the wide gap above the inner cylinder, which creates a thinner boundary layer on top of the outer cylinder. This is because of the availability of more space for circulation as the inner cylinder moves downward. From the flow pattern, it is observed that the center of the eddies on both sides of the inner cylinder moves closer with the increase in eccentricity. It is seen from the figure that the flow and thermal fields are symmetric about the vertical axis. When the inner cylinder is positioned upward, it is seen that the rising thermal plume gradually diminishes as observed from Figure 3(e) and (f). This happened because of the reduced air movements due to boundary layer inhibition at the extreme positions as the cylinders come closer. Therefore, near the

DOI: 10.1002/fld

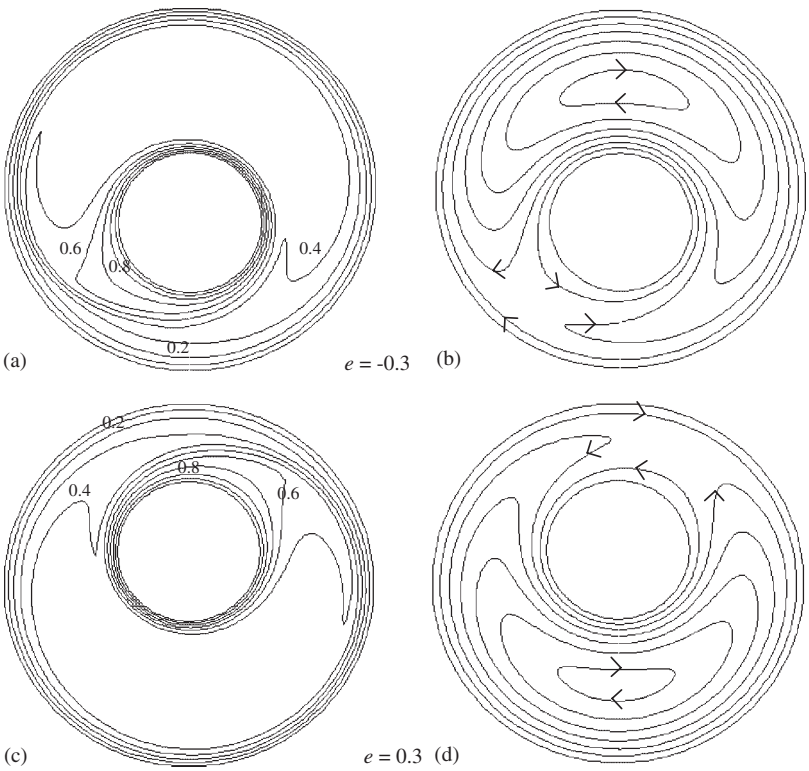

Figure 8. Isotherm and streamline pattern for mixed convection and radiation with variation in eccentricity (e) when $NR=1, \tau=1, \omega=0.5, \varepsilon=0.5, Ri=0.01, Ra=10^4$.

walls conduction bands exist. Furthermore, under the adverse effect of the recirculating vortices, the inflows toward the inner cylinder are suppressed.

The effect of radiation along with natural convection in the presence of participating media has been investigated for eccentricities i.e. $e=-0.3$ and 0.3 and is presented in Figure 4. Radiation redistributes the thermal energy and establishes an even distribution of energy in the domain, and in turn suppresses the convection plume rising from the inner cylinder as seen from the isotherm patterns. Looking at the streamline patterns, it is understood that, with the upward displacement of the inner cylinder, the center of circulation shifts downward.

Mixed convection and radiation

Isotherms and streamline contours are presented in Figure 5 for the case of pure mixed convection, varying Ri from 0.01 to 1 and eccentricity from -0.3 to 0.3 when $Ra=10^4$. At a low value of the Richardson number such as $Ri=0.01$, for a case of $e=-0.3$, the rising plumes from the inner cylinder shifted from the left to the bottom of the annuli. Looking at the streamlines, it is found that more packing of streams is observed at the upper portion of the annulus, which reflects stronger fluid circulation in that region. For the same value of Ri, looking at the case of $e=0.3$, it is observed that the center of circulation as well as the position of the rising plume from the inner

DOI: 10.1002/fld

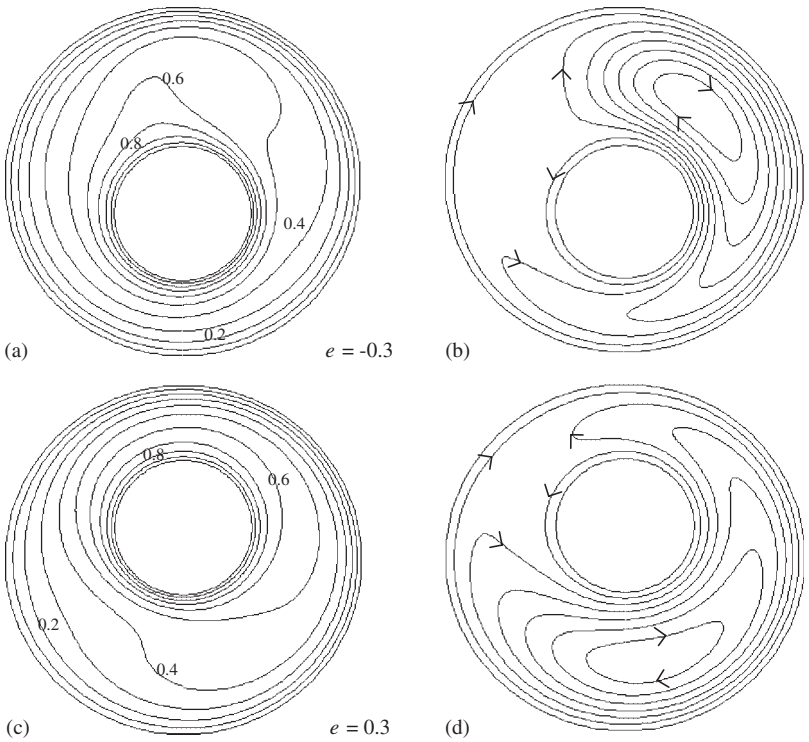

Figure 9. Isotherm and streamline pattern for mixed convection and radiation with variation in eccentricity (e) when $NR=1, \tau=1, \omega=0.5, \varepsilon=0.5, Ri=1,\ Ra=10^4$.

cylinder gets reversed completely compared with the previous case as shown in Figure 5. This is because of availability of space that helps in stronger fluid circulation and thereby drags the center of circulation toward the more available space. Figure 6 depicts the same phenomena but with the value of Richardson number as $Ri=1$. Here, almost the same outcome results with regard to the left half of the annuli, but on the right half, the center of circulation shifts downward as the inner cylinder moves upward. For both the eccentricities, the left portion of the annuli comes across a weak circulation. As a matter of fact, the conduction mode of heat transfer occurs in that portion of the annuli, as can be seen from the isotherm contours. From Table III, it can be seen that for both the eccentricities, the convective heat transfer is substantially higher for $Ri=0.01$ than for $Ri=1$, as expected. Moreover, it can be seen from Table III that beyond the range of '*Ri*', i.e. 0.01–1, further change in the value of '*Ri*' shows a negligible variation in the convective heat transfer process for all eccentricities. Thus, the further studies in the presence of radiation are conducted for the above-mentioned values of '*Ri*'.

Interaction of mixed convection with radiation in the presence of participating medium inside the eccentric annuli has been investigated for $Ri=0.01$ and 1, when the radiation–conduction parameter (NR) is set to 1 and $Ra=10^4$. No substantial changes occur in isotherm as well as in streamline contours for $Ri=0.01$ compared with the case of pure mixed convection as seen in Figure 7 This is also evident, as the '$\psi_{\max}$' value does not change with change in eccentricity

DOI: 10.1002/fld

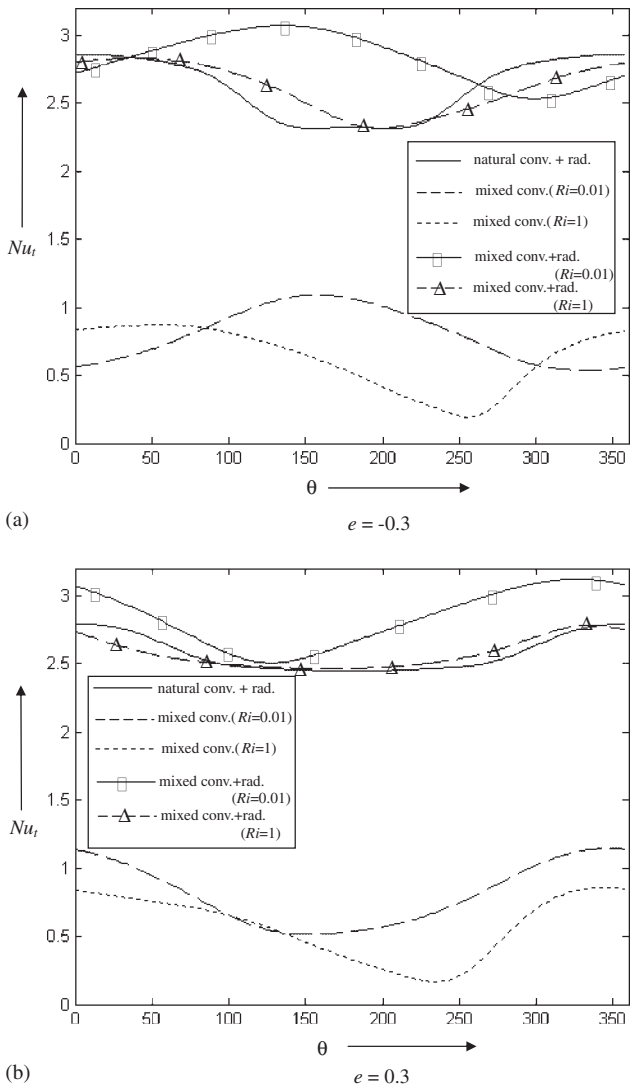

Figure 10. Variation in local total Nusselt number (Nu_t) along the inner cylinder wall for (a) $e=-0.3$ and (b) $e=0.3$ when $Ra=10^4$.

(Table IV). However, for the value of $Ri=1$, the changes in the contours are quite prominent, which can be seen from Figure 8. The maximum value of stream-function undergoes substantial change when the inner cylinder is in the upper half ($e=+0.3$). This implies that radiation induces some motion for this configuration. Here, due to the effect of radiation, the rising plume gets suppressed, which results in a decrease of convective current as compared with that of pure mixed convection case, i.e. at $Ri=1$. This is due to the fact that radiation redistributes the thermal energy made by pure mixed convection to set up a better thermal equilibrium condition inside the domain.

DOI: 10.1002/fld

The stagnant core still prevails in the left portion of the annuli for both the eccentricities $e=-0.3$ and 0.3, resulting in a conduction heat transfer there as seen from the isotherm contours. From Table IV, it can be seen that for both the eccentricities, the increase in radiative heat flux with respect to the decrease in the Richardson number (Ri) is quite marginal as compared with the increase in convective heat flux. Figure 9(a) and (b) represents the local total Nusselt number distributions along the inner cylinder wall for the values of eccentricity -0.3 and 0.3, respectively. From both the figures, it can be seen that the local total Nusselt number (Nu_t) distribution for the case of mixed convection and radiation attains a much higher value than the case of pure mixed convection. Thus, it can be understood that radiation plays a more dominant role with respect to energy transfer inside the domain (Figure 10).

In the above study, the eccentricity has been varied in the range of -0.3–0.3 for all the cases. To check the sensitivity of the amount of heat transfer toward eccentricity, a few computations are performed for eccentricities $e=-0.5$ and 0.5 but are not presented in the discussion. This is because the amount of heat transfer is found to vary with the eccentricity only in the case of pure natural convection. It remains almost invariant for the case of mixed convection and radiation, which can be easily seen in Table IV. In this table, it is clearly observed that the natural convection heat transfer increases continuously with the decrease in eccentricity (i.e. when inner cylinder moves downward), whereas almost insignificant variation can be noticed for the case of both mixed convection and radiation with change in eccentricity. As the above study is mainly focused on mixed convection in the presence of radiation, the range of eccentricity is restricted further.

CONCLUSIONS

The major conclusions drawn are outlined as follows:

- For $Ri=0.01$, the heat transfer is more compared with the same at $Ri=1$ in eccentric cylindrical annuli. However, for concentric cylindrical annulus, the heat transfer is minimum for $Ri=0.01$.
- Variation in eccentricity 'e' has a significant effect on pure natural convection heat transfer, whereas its effect is less pronounced for mixed convection and radiation.
- For an eccentricity of -0.3, the local total Nusselt number for the case of mixed convection and radiation gets maximized at a position of $\theta=150°$.

NOMENCLATURE

a	absorption coefficient of the medium (1/m)
A_i	area of the ith discrete surface on cylinder walls (m^2)
C_p	specific heat (J/kg K)
D	diameter of the cylinder (m)
d	$(D_o-D_i)/2$ (m)
e	eccentricity, y/d
g	gravitational acceleration (m/s^2)

DOI: 10.1002/fld

G	dimensionless irradiation
G_d	irradiation (W/m^2)
Gr	Grashof number, $g\beta\Delta T(r_o-r_i)^3/\nu^2$
h_i	$q_{wi}/(T_i-T_o)$
I^*	non-dimensional radiative intensity
k	thermal conductivity (W/m K)
K_{eq}	$h_i D_i \ln(r_o/r_i)/2k$
NR	radiation–conduction parameter ($r_i\sigma T_o^3/k$)
n	normal vector
Nu	Nusselt number
Pr	Prandtl number (ν/α)
q_w	heat flux per unit area from the cylinder surface
r	radial coordinate (m)
R	dimensionless radius (r/d)
Ra	Rayleigh number, $g\beta\Delta T(r_o-r_i)^3/(\nu\alpha)$
Re	Reynolds number, $u_0 d/\nu$
Ri	Richardson number, Gr/Re^2
s	space coordinate
T	temperature (K)
T_m	$(T_i+T_o)/2$ (K)
ΔT	temperature difference (T_i-T_o) (K)
u_0	linear velocity of the cylinder walls (m/s)
U	non-dimensional radial velocity component
V	non-dimensional azimuthal velocity component
W	weight factor used for discrete direction
y	vertical distance by which the inner cylinder is displaced (m)

Greek letters

α	thermal diffusivity (m^2/s)
ε	emissivity of the cylinder wall
ϕ	dimensionless temperature $(T-T_o/T_i-T_o)$
δ	overheat ratio $2(T_i-T_o)/(T_i+T_o)$
η	radius ratio (r_o/r_i)
θ	azimuthal coordinate
ν	kinematic viscosity (m^2/s)
σ	Stefan–Boltzmann constant ($W/m^2 K^4$)
σ_s	scattering coefficient of the medium (1/m)
ω	single-scattering albedo
τ	optical thickness $(r_o-r_i)(a+\sigma_s)$
ψ_d	stream-function (m^2/s)
ψ	dimensionless stream-function
Ω_d	vorticity (1/s)
Ω	dimensionless vorticity
ξ	scattering phase function (1/sr)
Φ	solid angle (sr)

DOI: 10.1002/fld

Subscripts

i	inner cylinder
o	outer cylinder
c	convection
r	radiation
t	total
w	wall
j	number of discrete directions

Superscripts

$'$	incoming direction

REFERENCES

1. Choudhury D, Karki KC. Laminar mixed convection in a horizontal eccentric annulus. *Numerical Heat Transfer A* 1992; **22**:87–108.
2. Fusegi T, Farouk B, Kenneth SB. Mixed convection flows within a horizontal concentric annulus with a heated rotating inner cylinder. *Numerical Heat Transfer* 1986; **9**:591–604.
3. Lee TS. Numerical computation of fluid convection with air enclosed between the annuli of eccentric heated horizontal rotating cylinders. *Proceedings of the International Conference on Scientific and Engineering Computations* 2002; **1**(3):355–368.
4. Lee TS, Hu GS, Shu C. Application of GDQ method for study of mixed convection in horizontal eccentric annuli. *International Journal of Computational Fluid Dynamics* 2004; **18**(1):71–79.
5. Taylor GI. Stability of viscous liquid contained between two rotating cylinders. *Philosophical Transactions of the Royal Society of London*, *Series A* 1923; **223**:289–343.
6. Coles D. Transition in circular Couette flow. *Journal of Fluid Mechanics* 1965; **21**:385–425.
7. DiPrima RC, Swinney HL. Instabilities and transition in flow between concentric rotating cylinders. In *Hydrodynamic Instabilities and the Transition to Turbulence*, Swinney HL, Gollub JP (eds). Springer: New York, 1985; 139–186.
8. Ball KS, Farouk B. On the development of Taylor vortices in a vertical annulus with a heated rotating inner cylinder. *International Journal for Numerical Methods in Fluids* 1987; **7**:857–867.
9. Ball KS. Mixed convection heat transfer in rotating system. *Ph.D. Thesis*, Department of Mechanical Engineering and Mechanics, Drexel University, 1987.
10. Chui EH, Raithby GD. Computation of radiant heat transfer on a non-orthogonal mesh using finite-volume method. *Numerical Heat Transfer* 1993; **23**:269–288.
11. Chai JC, Lee HS, Patankar SV. Finite-volume method for radiation heat transfer. *Journal of Thermophysics* 1994; **8**:419–425.
12. Kim MY, Baek SW. Numerical analysis of conduction, convection and radiation in a gradually expanding channel. *Numerical Heat Transfer* 1996; **29**:725–740.
13. Onyegegbu SO. Heat transfer inside a horizontal cylindrical annulus in the presence of thermal radiation and buoyancy. *International Journal of Heat and Mass Transfer* 1986; **29**:659–671.
14. Mahapatra SK, Nanda P, Sarkar A. Interaction of mixed convection in two sided lid-driven differentially heated square enclosure with radiation in presence of participating medium. *Journal of Heat and Mass Transfer* 2006; **42**:739–757.
15. Tan Z, Howell JR. Combined radiation and natural convection in a participating medium between horizontal concentric cylinders. In *Heat Transfer Phenomena in Radiation*, *Combustion and Fires*, Shah RK (ed.). ASME: New York, 1989; 87–94.
16. Morales JC, Campo A. Radiative effects on natural convection of gases confined in horizontal, isothermal annuli. In *Developments in Radiative Heat Transfer*, Thynell ST *et al*. (eds). ASME: New York, 1992; 231–238.

DOI: 10.1002/fld

17. Burns SP, Howell JR, Klein DE. Application of the finite element method to the solution of combined natural convection–radiation in a horizontal cylindrical annulus. In *Numerical Methods in Thermal Problems*, Lewis RW, Durbetaki P (eds), vol. IX. Pineridge Press: Swansea, U.K., 1995; 327–338.
18. Gebhart B, Jaluria Y, Mahajan R, Sammakia B. *Buoyancy Induced Flows and Transport*. Hemisphere Publishing Corporation: New York, 1988; 764–771.
19. Modest MF. *Radiative Heat Transfer* (1st edn). McGraw-Hill: New York, 1993; 559–567.
20. Kuo DC, Morales JC, Ball KS. *Combined Natural Convection and Volumetric Radiation in a Horizontal Annulus*: *Spectral and Finite Volume Predictions*, vol. 121. ASME: New York, 1999; 610–615.
21. Kuehn TH, Goldstein RJ. An experimental study of natural convection heat transfer in concentric and eccentric horizontal cylindrical annuli. *Journal of Heat Transfer* (ASME) 1978; **100**:635–640.

DOI: 10.1002/fld